ORIGINAL ARTICLE

Comparing CW-GMAW in direct current electrode positive (DCEP) and direct current electrode negative (DCEN)

P. D. C. Assunção[1] · R. A. Ribeiro[2] · E. B. F. Dos Santos[3] · E. M. Braga[1] · A. P. Gerlich[2]

Abstract

Gas metal arc welding (GMAW) with direct current electrode negative (DCEN) can offer some advantages over direct current electrode positive (DCEP) welding, such as a higher electrode melting rate and lower heat input imposed onto the workpiece. Despite these advantages, DCEN is not commonly used in field applications due to instabilities caused by arc climb and the volatile repelled metal transfer mode across the arc. This work reports a comparison between DCEP and DCEN in natural spray transfer mode using a welding power source operating in constant voltage (CV). It aims to assess the feasibility of DCEN in cold wire gas metal arc welding (CW-GMAW) comparing the results obtained in DCEN with previous results obtained in DCEP for the same welding parameters. During experiments, the current and voltage were acquired with synchronized high-speed video to study the arc dynamics. Bead-on-plate welds were deposited onto AISI 1020 steel flat bars. Three cross sections for each bead were cut and metallographically examined to compare bead geometry. Results suggest that the cold wire feeding can suppress arc climb in DCEN welding, consequently improving the arc stability and bead finish. Moreover, the DCEN welds suggest that the heat transferred to the weld pool is fundamental to accommodate high feed rates of cold wire. Lastly, the cross section results show that penetration, dilution, and HAZ area are lower in DCEN than in DCEP mode.

Keywords DCEP · DCEN · GMAW · CW-GMAW · Arc climbing · Bead geometry · Dilution

1 Introduction

The use of direct current electrode negative (DCEN) in welding offers two major advantages when compared with direct current electrode positive (DCEP), namely, the higher melting rate and the low heat imposed onto the substrate. However, these two potential advantages are impaired by the repelled metal transfer and the arc climb that occur in DCEN.

Consequently, welding with DCEN seems to be neglected in the literature and is not applied in commercial applications.

✉ R. A. Ribeiro
   rdearauj@uwaterloo.ca

1   Metallic Materials Characterization Laboratory (LCAM), Federal University of Pará (UFPA), Rua Augusto Corrêa, 1 - Guamá, Belém, PA 66075-110, Brazil

2   Centre for Advanced Materials Joining (CAMJ), University of Waterloo, 200 University Avenue West, Waterloo, ON N2L 3G5, Canada

3   Liburdi Automation Inc. - Liburdi GAPCO, 400 ON-6, Dundas, ON L9H 7K4, Canada

However, with the development of new power sources and a better understanding of the role of shielding in welding, studies have begun to analyze some welding characteristics offered by DCEN. For example, perhaps one of the first papers to state the feasibility of welding in DCEN was by Norrish [1], which indicated the general feasibility of the technique but just for limited applications.

Souza et al. [2] proposed a qualitative model to explain the higher melting rate in DCEN for different shielding gas mixtures; the main conclusion was that arc climb is responsible for improved melting rates. Later research by the same group used DCEN in a double-wire (tandem GMAW) configuration to investigate the effects of different polarities in leading and trailing wires. The main conclusion was that the use of DCEN in the trail wires increases the productivity but decreases the operational range of process parameters.

Recently, Li et al. [3] evaluated bead-on-plate welds with DCEN using different shielding gases and obtained spray transfer mode. They reported that the best results were obtained with Ar-6.5% O_2. Also recently, the interest in variable polarity gas metal arc welding (VP-GMAW) has increased, since it can control the heat input to the substrate and allow

Table 1 Nominal chemical composition base metal and welding wire

Material	Nominal chemical composition (wt%)						
	C	Si	Mn	P	S	Cr	Fe
AISI 1020	0.18	–	0.3	Max. 0.040	Max. 0.05	–	Balance
ER70S-6	0.15	1.15	1.85	0.025	0.035	0.05	Balance

the welding of heat-sensitive materials [4]. Moreover, the interest in alternating current GMA welding is based on its potential higher productivity coupled with reduced nominal heat input. Kim and Chung [5] estimated the fusion rate coefficients for AC square current wave form and concluded that the melting rate is not only a function of polarity but also a function of of droplet shape and current waveform.

The value in increasing productivity without an increase in heat input has led some researchers to focus on cold wire gas metal arc welding (CW-GMAW), which involves feeding a non-energized wire (cold) into the weld pool. Prior research has shown that this process promotes a decrease in thermal distortion [6] in welding of large panels for naval applications. Subsequently, Costa [7] has shown that the process imposed less residual stresses than the standard GMAW welded with the same parameters. Also, this decrease in residual stresses might offer superior fatigue life for CW-GMA-welded joints compared with GMA-welded joints [8].

Considering that the information available in the literature seems to characterize the DCEN variant of GMAW as a promising technique with improved productivity and rather simple operational setup, however, few studies are found involving a direct comparison to DCEP, and some are even contradictory. The purpose of the present work is to offer a contribution to the debate on DCEN GMA welding, whereas most available research concentrates on constant current and complex waveforms for DCEN. This work uses constant current (CV) as this type of source is more common in practical applications. In addition, to the authors' best knowledge, the discussion on CW-GMA welding with negative polarity is presented for the first time in this work.

2 Methodology

In order to assess the arc behaviour and bead features, bead-on-plate welds were deposited onto hot-rolled AISI 1020 steel flat bars measuring 190.5 mm (7.5 in.) × 50.8 (2 in.) × 9.525

(3/8 in.). ER70S-6 was used as electrode wire (1.2 mm) and as cold wire (0.9 mm). Table 1 gives the nominal chemical composition of the base metal and welding wire according to references [9, 10], respectively.

A Lincoln R500 was used to perform the welds in constant voltage mode (CV) both for direct current electrode positive (DCEP) and for direct current electrode negative (DCEN). An external Lincoln wire feeder was used to feed the cold wire (CW) in both polarities. For all welds, the shielding gas employed was Ar-15% CO_2 at a flow rate of 17 l/min (40 ft^3/h) and the contact tip to workpiece distance (CTWD) was kept at 17 mm for all welds. The natural transfer mode of spray was chosen to allow a better visualization of the arc phenomena, especially in DCEN.

In order to assess the arc dynamic behaviour current and voltage, they were measured using a LEM LF 505-S and a LEM LV 100 sensors with reported accuracy of ± 0.6% and ± 0.9%, according to the manufacturer, respectively [11, 12]; the current and voltage signals were discretized at 16 bits using a NI 6002 DAQ system with a frequency of 10 kHz for 2 s. In parallel, high imaging synchronized to current and voltage probing was used to analyze the arc dynamics. The reported values of current, voltage, and power were calculated using the instantaneous average value as recommended in prior work [13]. The image acquisition was performed at 5000 fps with a shutter speed time of 25 μs and band pass filter of 900 ± 10 nm. The welding parameters set in the power source for both polarities are presented in Table 2.

The CW was fed in percentage rates based on the mass deposition rate fed through the electrode wire. These percentages were calculated from the wire feed speed considering the density of the wire electrode equal to 7930 kg/m^3 and calculating its cross-sectional area. CW feed rates of 40%, 60%, and 80% were employed in this work. Figure 1 shows the experimental setup used in the experiments and the detail regarding the cold wire feeding angle. The welding direction was from the left (yellow arrow) to the right.

After welding, the beads were photographed and cut in three cross sections in order to evaluate the geometrical features. The cross sections were subjected to standard metallographic procedure and etched with Nital (2%). Then, the geometric features, namely penetration depth, bead height, bead width, cross-sectional area, dilution, heat-affected zone (HAZ) area, and wetting angle (θ), were measured. Figure 2 shows a schematic of one cross section indicating how the geometric features reported in this work were measured.

Table 2 Welding parameters set in the welding source

Wire feed speed (in/min) [m/min]	Voltage (V)	Travel speed (in/min) [cm/min]
350 [8.89]	30	25 [63.5]

Fig. 1 Experimental setup used to manufacture the welds. (a) General view, the index finger indicates the ground of the welding source. (**b**) Detail of the cold wire angle. The yellow arrow indicates where the source negative cable was put
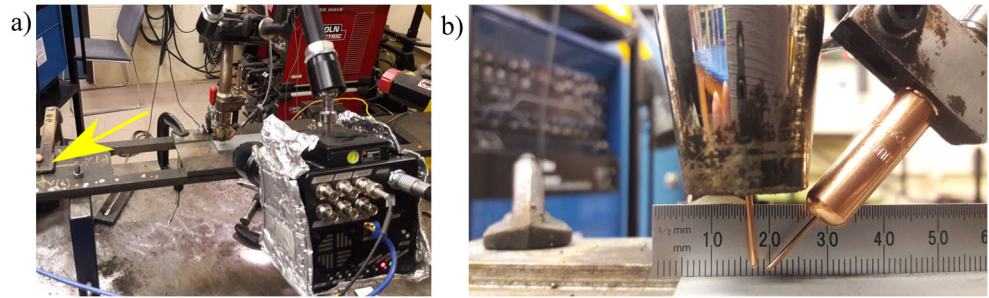
3 Results and discussions

3.1 Electrical data

The voltage standard deviation (STD) values calculated from the sampled voltage during welding are presented in Fig. 3. One of the issues reported in the literature regarding welding with DCEN is the stability of the electric arc [14]. Assuming that the electric is an *ER* circuit, where *E* represents the potential drop across the source, cabling, and wire and *R* is the overall arc resistance. The voltage measured between the torch and the substrate can be modelled according to Kodama et al. [14] as:

$$U_a = U_{a0} + R_a I + E_a l_a \qquad (1)$$

where U_a (V) is the voltage measured, U_{a0} (V) is a constant component of voltage, R_a (Ω) is the arc column, E_a (V/m) is the electric field in the arc column, and l_a (m) is the arc length. Arc stability relies on a uniform arc length during welding operation to ensure stable metal transfer without spatter. Thus, one can relate stability to measurable arc voltage assuming that all parameters remain constant. Considering the voltage STD for DCEP, it appears that the introduction of cold wire does not detrimentally affect the stability of the process, taking the measured voltage in GMAW as a standard. On the contrary, it seems that the introduction of cold wire might even be beneficial to arc stability as can be seen by the standard deviation of average voltage for 80% cold wire feeding. The voltage standard deviation in DCEP (Fig. 3a) for the standard GMAW is 0.44 V versus 0.31 V for CW-GMAW-80% which indicates the improved stabilization. In DCEN, the voltage standard deviation of GMAW is 1.5 V versus 1.38 V for CW-GMAW-80% as can be noted in Fig. 3b.

The data presented in Fig. 3 suggest that the cold wire in DCEP and DCEN may play a role in the arc stabilization. In order to determine if this is the case, one can employ the following model proposed by Hajossy and Morva [15], in which the voltage over time:

$$U(t) = U_c + U_a + U_{col}(t) \qquad (2)$$

where U_c is the cathode voltage fall in volt, U_a is the anode voltage fall in volt, and $U_{col}(t)$ is the arc column voltage fall in volt. The cathode and anode voltage falls are constant in time. However, the arc column is dependent on time and proportional to arc length. Wherefore, one can write:

$$\frac{dU(t)}{dt} = \frac{dU_{col}(t)}{dt} = k \frac{dl_a}{dt} \qquad (3)$$

where $\frac{dU(t)}{dt}$ is the instantaneous voltage variation in volt per millisecond, $\frac{dU_{col}(t)}{dt}$ is the arc column voltage fall instantaneous variation in volt per millisecond, $\frac{dl_a}{dt}$ is the instantaneous variation of arc length (mm/ms), and k is the proportionality constant between $\frac{dU_{col}(t)}{dt}$ and $\frac{dl_a}{dt}$ in volt per millimetre. One can notice that based on the units, k is simply the electric field strength inside the arc column. Thus, plotting $\frac{dU(t)}{dt}$ for all conditions in this work is a means of assessing arc stability.

Figure 4 shows the range of the instantaneous voltage variation (V/ms); one should note that that lower range of variation correlates to better arc stability. The range was calculated as:

$$\text{Range} = \left(\frac{dU(t)}{dt}\right)_{max} - \left(\frac{dU(t)}{dt}\right)_{min} \qquad (4)$$

where $\left(\frac{dU(t)}{dt}\right)_{max}$ is the maximum value of the instantaneous voltage variation and $\left(\frac{dU(t)}{dt}\right)_{min}$ is the minimum value of instantaneous voltage variation.
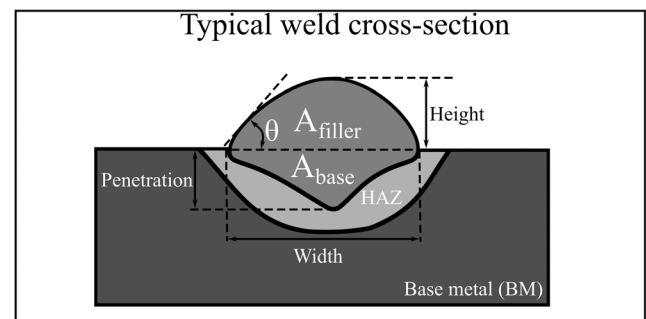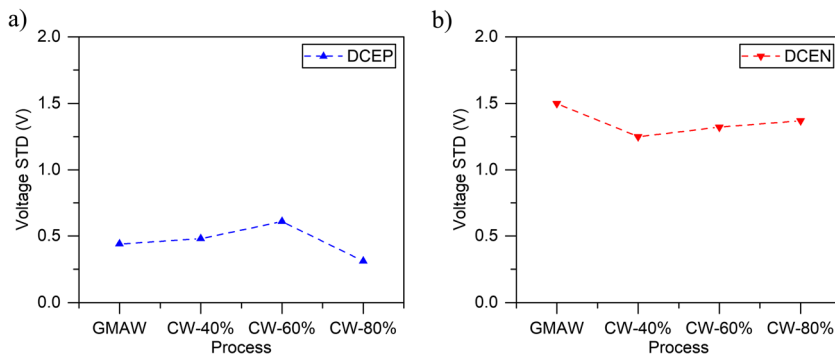

Fig. 2 Schematic of a cross section showing how the geometric features were measured

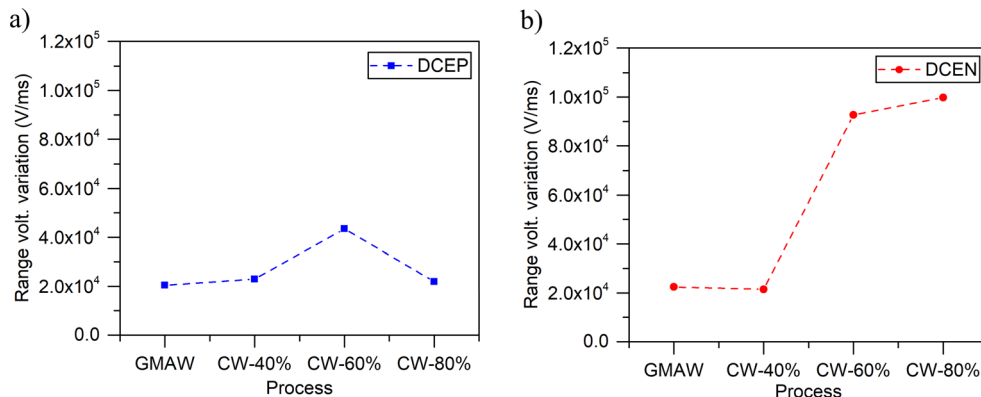**Fig. 3** Voltage standard
deviation. (a) DCEP. (b) DCEN

For DCEP (Fig. 4a), the progressive introduction of cold wire leads to progressive instability until a cold wire feed rate of 60%. Then, with 80%, the range is in the order of magnitude of GMAW. This is consistent with progressive pinning of the arc to the cold wire for increasing cold wire feed rates; further details can be found in Ribeiro et al. [16].

However, for DCEN (Fig. 4b), the progressive introduction of higher cold wire feed rates leads to instability of the arc with cold wire fractions higher than 40%. This is consistent with the results presented in Fig. 9 (showing the cyclogrammes for DCEN) in which one can note the same trend.

According to Kim and Chung [5] and Cary [17], there is less heat input transferred to the base metal using DCEN, with accounts for less penetration. This is consistent with what is shown in Fig. 16a, where for the same welding parameters, the penetration in DCEN is always less than that in DCEP. The summary of electrical data sampled during welding can be seen in Fig. 5. Again one can see that in DCEN, the average voltage is higher than in DCEN which indicates a higher arc length in DCEN, for the same welding parameters. The same trend is observed in the effective voltage (voltage RMS); in DCEN, the RMS voltage is higher than in DCEP.

Moreover, the average power in DCEN considering all conditions is 8223 W while the average for all conditions in DCEP is 8824 W. Thus, the power in DCEN is 6.8% less than that in DCEP which can be seen in Fig. 5 e and f.

3.2 Oscillograms and cyclogrammes

Fig. 6 shows the oscillograms of the welds performed in DCEP. Again, one can see that over the collected period, the influence of cold wire evolves from a perturbation which can be seen from the data compared for CW-GMAW-40% (Fig. 6b) to CW-GMAW-60% (Fig. 6c) in the form of ripples, which are absent in the data for CW-GMAW-80% (Fig. 6d).

The rationale to explain the effect of cold wire on the welding stability in DCEP must be assessed by high-speed imaging of the arc, as will be discussed in Section 3.3. The repelled metal transfer and the arc climbing are the main contributors to perturbations during DCEN welding (Fig. 7) which can be noticed by the peaks in the oscillograms. Another feature that can be noted in the oscillograms is that spray metal transfer dominates. Some previous research stated that welding in DCEN in spray was not practical and should be under mildly oxidative shielding mixture [18].

In order to corroborate the statements regarding the arc stability promoted by cold wire feeding in DCEP, cyclogrammes which are plots of voltage versus current can be used to analyze the behaviour of the arc over all the sampled period (refer to Fig. 8).

One can see that the standard GMAW condition provides a stable spray condition with the arc staying around the pre-set voltage condition at least 10% of the sampling time (Fig. 8a). As the cold wire starts being fed, there is a displacement
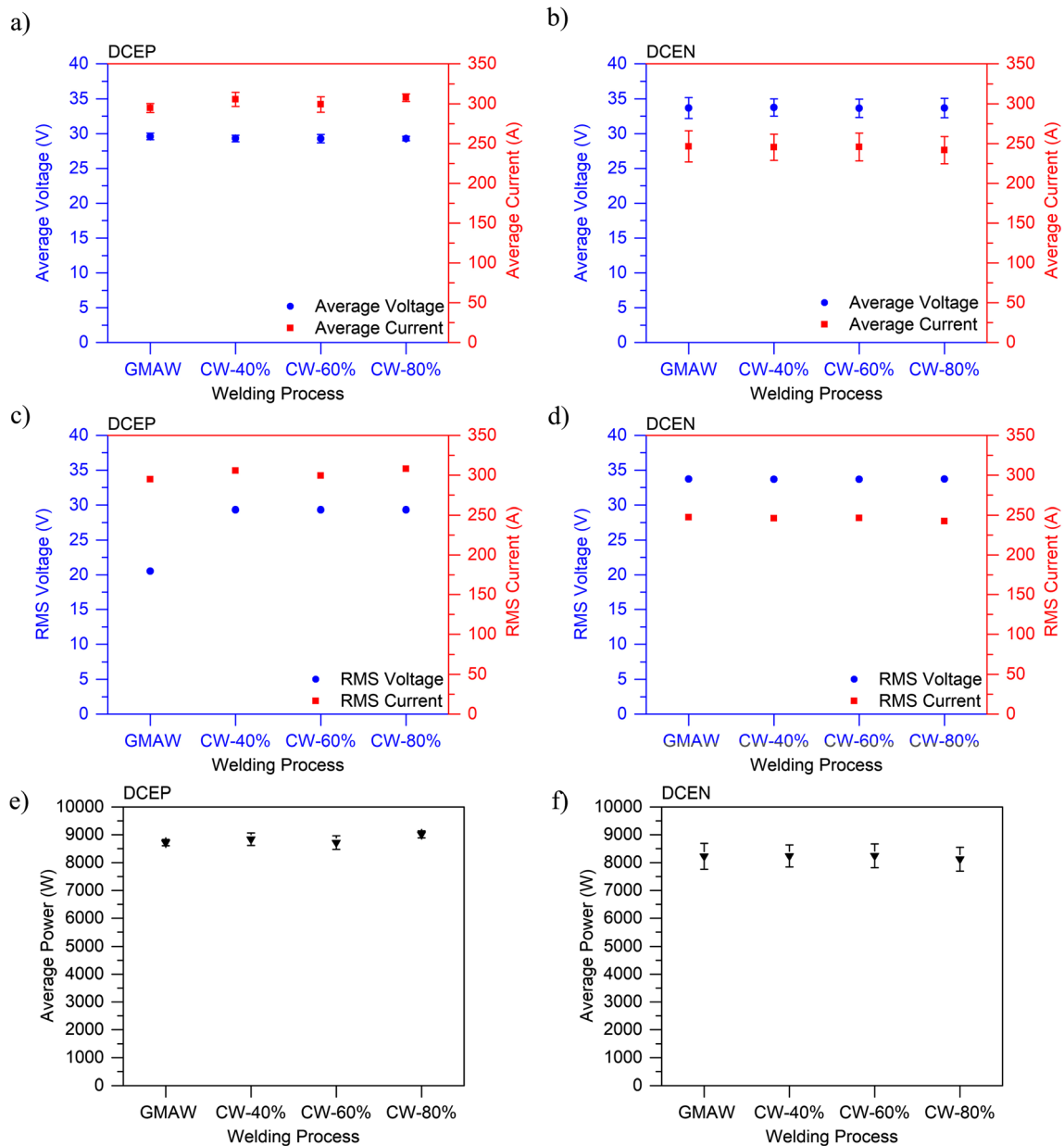
Fig. 4 Range of instantaneous
voltage variation. (a) DCEP. (b)
DCEN

Fig. 5 Summary of the electrical data for all the conditions. (a, b) Instantaneous average voltage and current. (c, d) RMS voltage and current. (e, f) Instantaneous power

towards the direction of higher currents; Ribeiro et al. [16] described this phenomenon, which is probably related to the arc self-regulation in CV, slightly increasing the current to melt more material. One discerns that there is a decrease in the frequency of the arc around the set point of voltage, which is probably due to the disruption that the cold wire has when forcing the arc to search for a new stable and equivalent set point (see Fig. 8b).

In Fig. 8c, one can see that frequency around the set point increased again but at the cost of high variations in current. Conversely, when a cold wire feed ratio of 80% is reached, the region describing the arc point combinations during welding decreases and a new stable point is achieved reflected on the

slightly decreased value of average voltage 29.30 V (Fig. 8d). The mechanism behind that stabilization in DCEP is described elsewhere [16].

Figure 9 shows the cyclogrammes for DCEN and one can clearly see the difference in standard GMAW. The arc is displaced towards regions of higher voltage and lower current, consequently displacing the dynamic set point of the arc to slightly higher averages (refer to Fig. 9a). Comparing Fig. 9a and Fig. 9b, one can see that there is a slight decrease of the arc operation region, though a decrease in frequency around the set point is observable. This effect was found to be restricted to a cold wire feed rate of 40%. With feed rates of 60% and 80%, the introduction of cold wire promotes short circuits
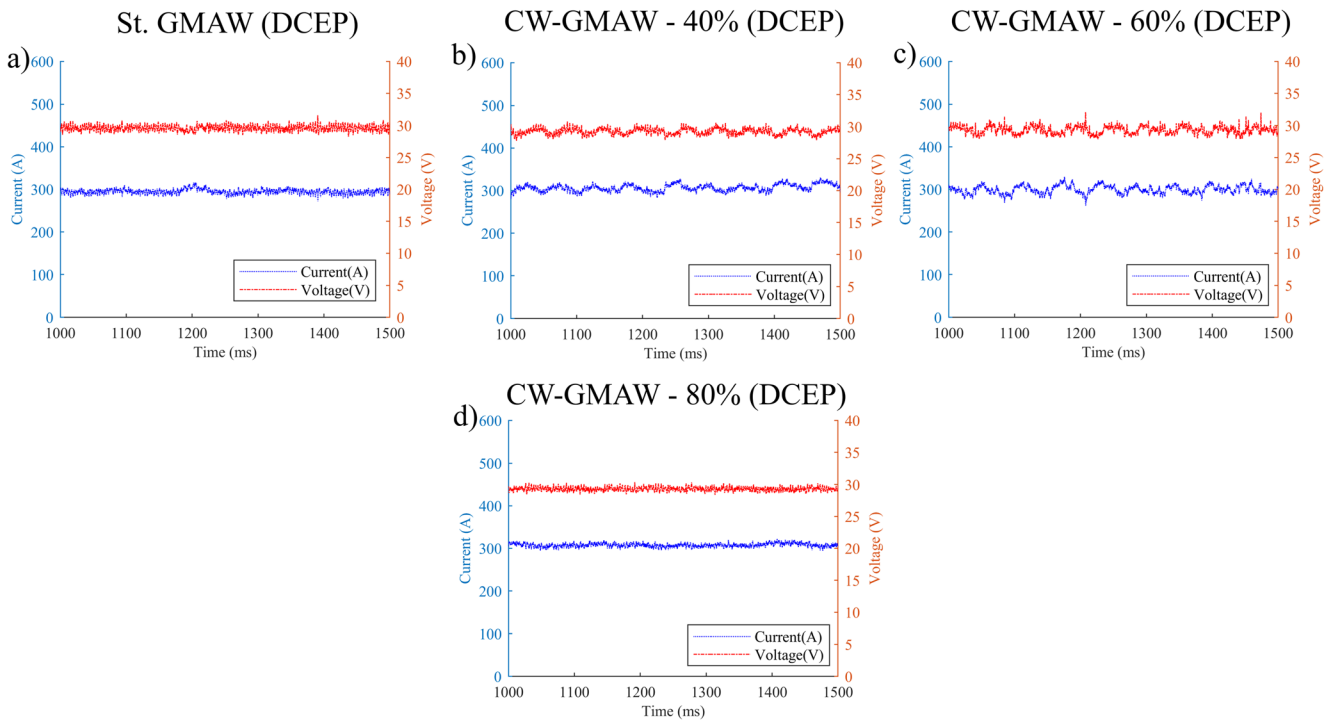
Fig. 6 Oscillograms for welds performed with positive polarity (DCEP). (a) St. GMAW (DCEP). (b) CW-GMAW-40% (DCEP). (c) CW-GMAW-60% (DCEP). (d) CW-GMAW-80% (DCEP)

increasing the arc wandering around the set point, consequently, augmenting the arc instability. However, the frequency around the set point increases (refer to Fig. 9 c and d respectively).
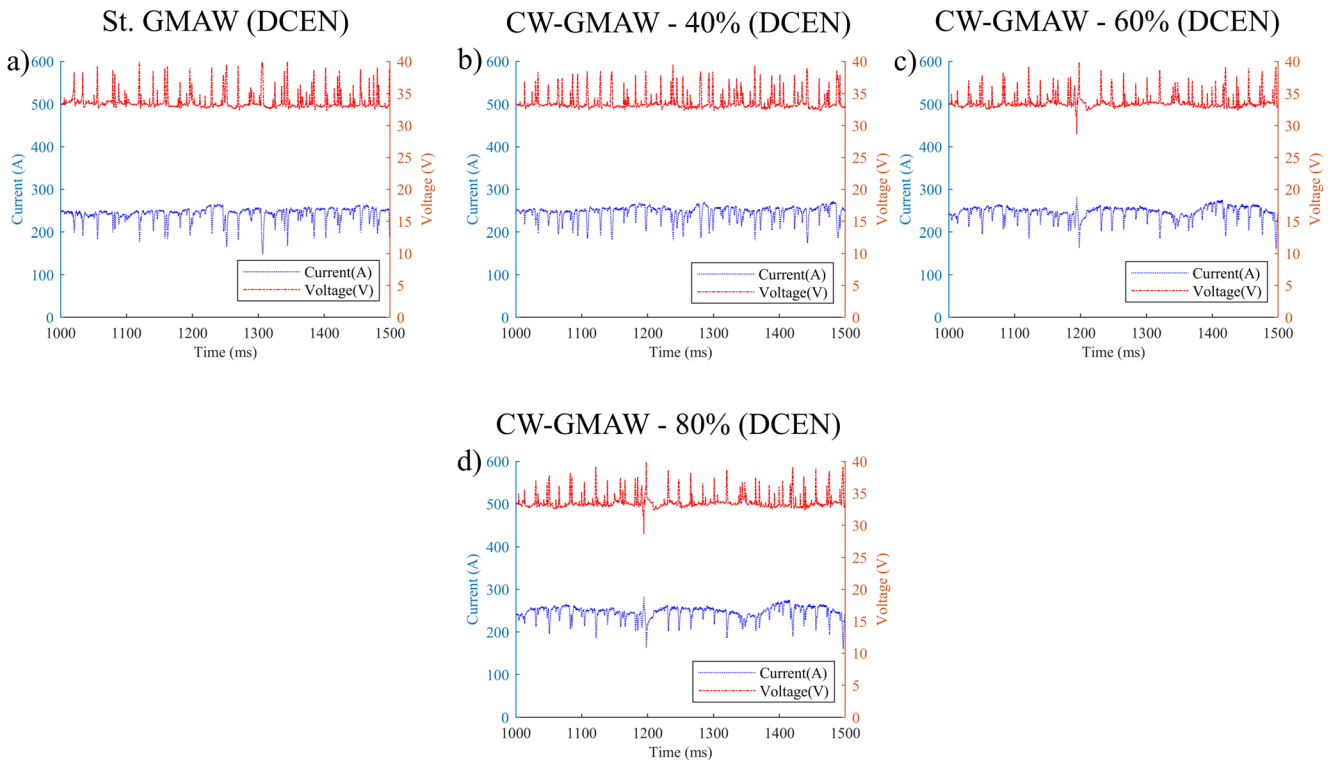

Fig. 7 Oscillograms for welds performed with negative polarity (DCEN). (a) St. GMAW (DCEN). (b) CW-GMAW-40% (DCEN). (c) CW-GMAW-60% (DCEN). (d) CW-GMAW-80% (DCEN)

Fig. 8 Cyclogrammes for welds in DCEP, scale indicates density of data points. (a) DCEP-GMAW. (b) DCEP-CW-GMAW-40%. (c) DCEP-CW-GMAW-60%. (d) DCEP-CW-GMAW-80%
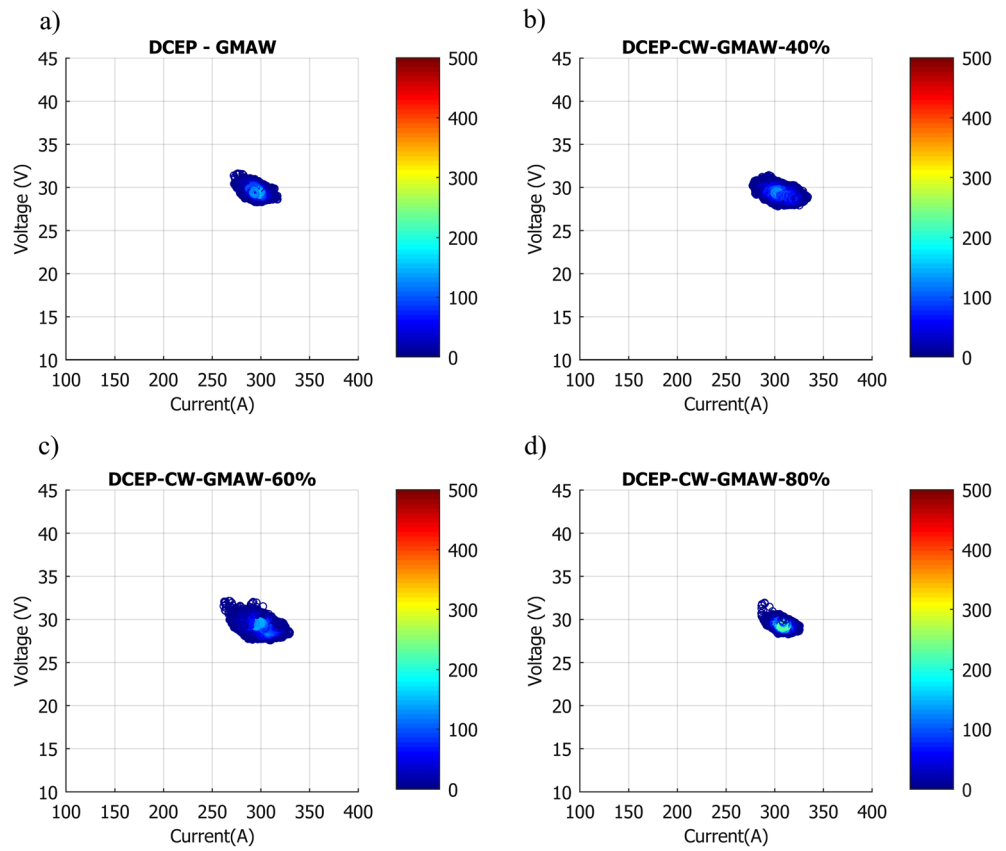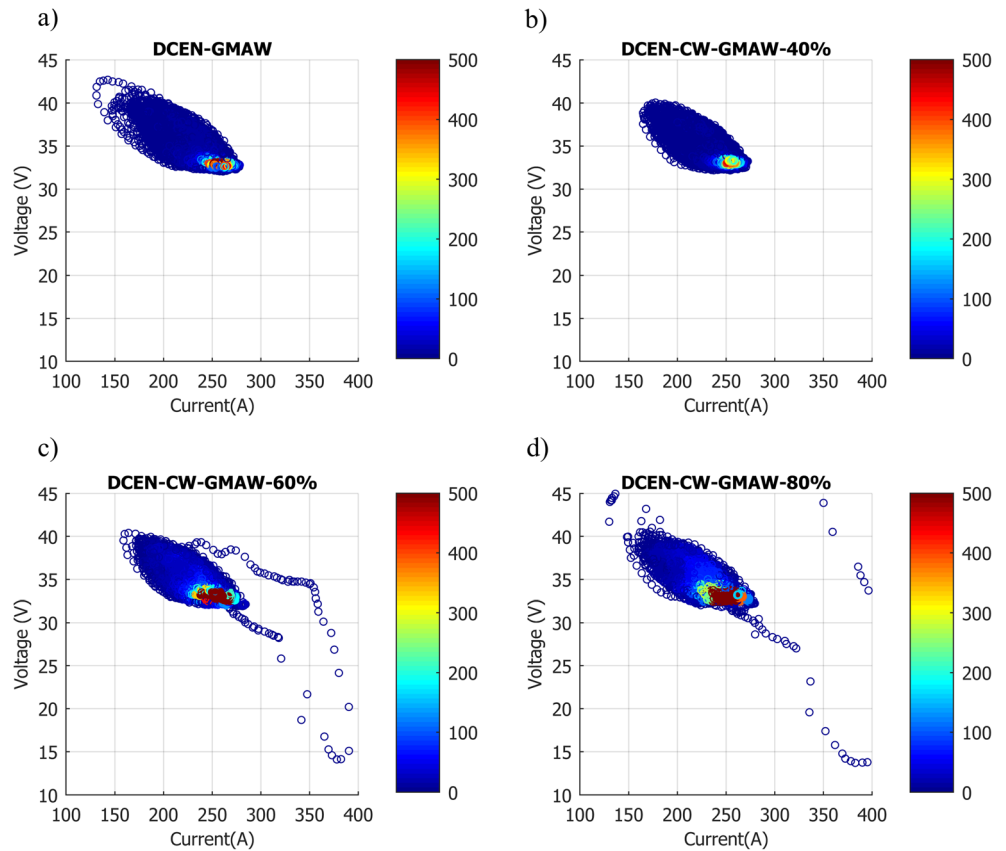

Fig. 9 Cyclogrammes for welds in DCEN, scale indicates density of data points. (a) DCEN-GMAW. (b) DCEN-CW-GMAW-40% (DCEN). (c) DCEN-CW-GMAW-60%. (d) DCEN-CW-GMAW-80%
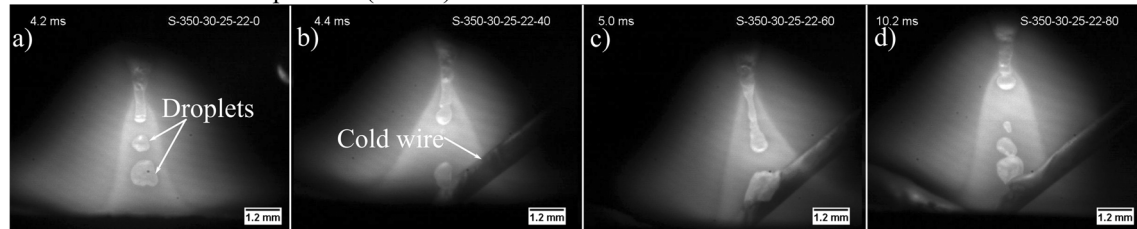
Direct current electrode positive (DCEP)

Fig. 10 Metal transfer with the electrode positive. (a) Standard GMAW. (b) CW-GMAW-40%. (c) CW-GMAW-60%. (d) CW-GMAW-80%

3.3 High-speed imaging of arc behaviour

In this section, the mechanism behind the cold wire stabilizing effect in DCEP will be discussed in some detail. One can see in Fig. 10 that as the cold wire feeding increases, the arc climbs the cold wire; in this condition, there is a slight decrease arc length confirmed by a slight decrease in average voltage measured during the welds. This decrease in arc length is reflected by the arc stability, since the value of voltage will not vary significantly around the pre-set value in the source as it is operating in constant voltage. Comparing the behaviour of the arc in DCEP and DCEN, one can see that the arc climbs the electrode wire, so that is now rooted inside the torch as indicated by Fig. 11a.

As the cold wire is introduced, the phenomenon arc pinning to the auxiliary wire (cold wire) is still observable and this phenomenon slightly stabilizes the arc, bringing the arc down while increasing the deposition. One can see the cathode spots observed on the hanging droplet in Fig. 11c, where the electrons emitted from it cause a reaction force, causing the droplet to detach asymmetrically. Contrary to the expected behaviour, the asymmetry in detachment is not as pronounced. When the cold wire feed reaches 80%, it was noted that the arc is prone to climb again, as suggested by the cyclogrammes.

As in the case of DCEN, there is less energy transferred to substrate/weld pool and the heat is insufficient to fully melt the cold wire. In this situation, the cold wire is deflected by the action of the heat in the weld pool, and eventually can touch droplets still attached to the electrode wire. This phenomenon is illustrated in Fig. 12 where the arrow indicates the cold wire position until it touches the droplet column causing short

circuit. In DCEP, this situation is not possible since there is enough heat in the weld pool to completely melt the cold wire.

3.4 Bead aspect and cross sections

Fig. 13 and Fig. 14 show the bead aspects for DCEP and DCEN, respectively. The weld bead convexity can be inferred from the bead geometry, since wider beads have low convexity angles while narrower beads have high convexity angles. By comparing DCEP with DCEN beads, one can note the last ones are more convex, as expected; this involves reduced heat transferred to the plate. Other fact that can be inferred is that the heat transferred to the weld pool is fundamental to the accommodation of cold wire feed. One can see in Fig. 13d and Fig. 14d that for the same welding parameters, the resulting morphology of the welding bead is completely different. For example, when using DCEN, a maximum feed rate of 60% cold wire is achievable while still providing a suitable weld bead; however, the amount of spatter is considerable. Then, one may expect that 40% is the real limit of cold wire feed rates to meet both bead finishing and spatter requirements.

Overall, all the welds did not present superficial cracks of any sort, where no porosity and no undercuts were detected by visual inspection. In all the cold wire welds, the volume of the welding pool increased significantly compared with its counterpart standard GMAW in DCEP and DCEN polarities, as expected due to an increase in deposition through cold wire feeding.

One can notice through the cross sections that none of the welding conditions presented internal porosities, cracks, or

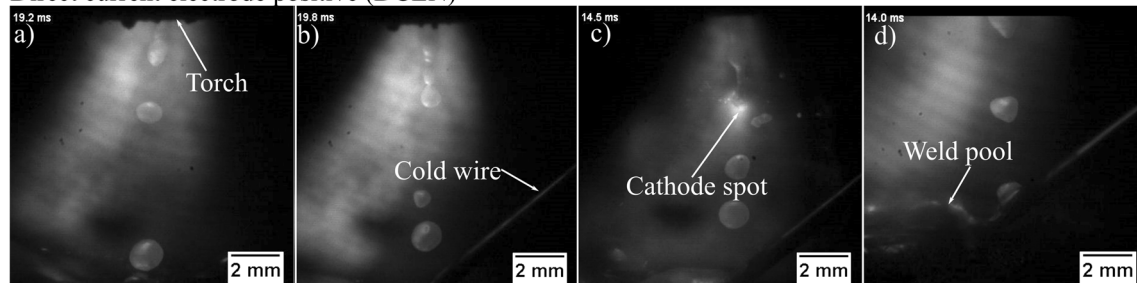Direct current electrode positive (DCEN)

Fig. 11 Metal transfer with the electrode negative. (a) Standard GMAW. (b) CW-GMAW-40%. (c) CW-GMAW-60%. (d) CW-GMAW-80%
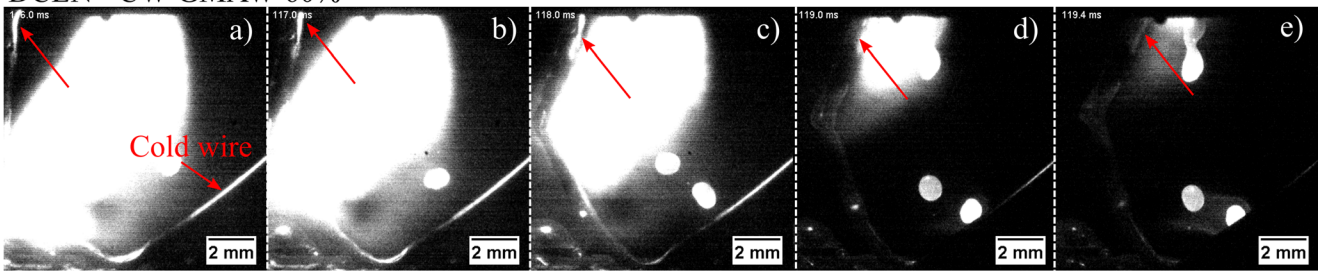
DCEN - CW-GMAW-60%

Fig. 12 Short-circuit phenomena in CW-GMAW-60% operating in DCEN. The red arrow indicates the tip of the cold wire

lack of fusion. The reduction in penetration due to increasing the CW ratio is more pronounced in DCEN than in DCEP. The mechanics of penetration will be treated in the next section. Another feature is that in DCEP, the finger-like penetration characteristic of spray transfer is not supressed even at a cold wire feeding rate of 80% (Fig. 15d). On the contrary, this observable trend in standard GMAW using DCEN is reduced at a 40% cold wire feed rate (Fig. 16b), but not completely supressed either. Ribeiro et al. [16] have shown that the alleviation of the finger profile in DCEP occurs only in higher cold wire feed rates. This difference suggests that difference in heat transfer to the workpiece and polarity plays a role in the finger profile reduction.

3.5 Bead geometry and dilution

Penetration in a simple model proposed by Murray and Scotti is a function of the thermal energy that triggers the temperature-dependent convection in the weld pool, and of the mechanical excavation performed by droplet momentum. Both effects can be summarized into two dimensionless factors. In the original work by Murray and Scotti [19], those were called A, the dimensionless mass transfer number which accounts for

the mechanical effect of droplets, and B, the dimensionless heat transfer number which accounts for the thermal effect of penetration. It is important to mention that a full description of mechanisms involving penetration and the interplay of these dimensionless parameters are out of the scope of this paper.

The dimensionless heat transfer was defined earlier by Fuerschbach [20] as the Rykalin number (Ry), to honour the late N. N. Rykalin. According to Mendez, Lu, and Wang [21], this quantity defines two types of behaviour of the welding heat source, namely, a slow heat source and fast source. However, the application of this quantity relies on an estimate of the thermal efficiency for cold wire welding, and this is not available in the literature.

One can see in Fig. 17a that the decrease in penetration was steeper in DCEN than in DCEP. This is probably due to the reduced heat dissipation into the welding pool in DCEN. Another feature is that the decrease in penetration might be due to the mechanical action of the cold wire acting as a barrier to the droplet momentum as can be seen in Fig. 11d. In fact, droplet mechanical effect on penetration is quantified by the droplet momentum, as described in the work of Scotti and Rodrigues [22].

Fig. 13 Bead aspects for positive polarity. (a) Standard GMAW. (b) CW-GMAW-40%. (c) CW-GMAW-60%. (d) CW-GNAW-80%

Fig. 14 Bead aspects for negative polarity. (a) Standard GMAW. (b) CW-GMAW-40%. (c) CW-GMAW-60%. (d) CW-GNAW-80%
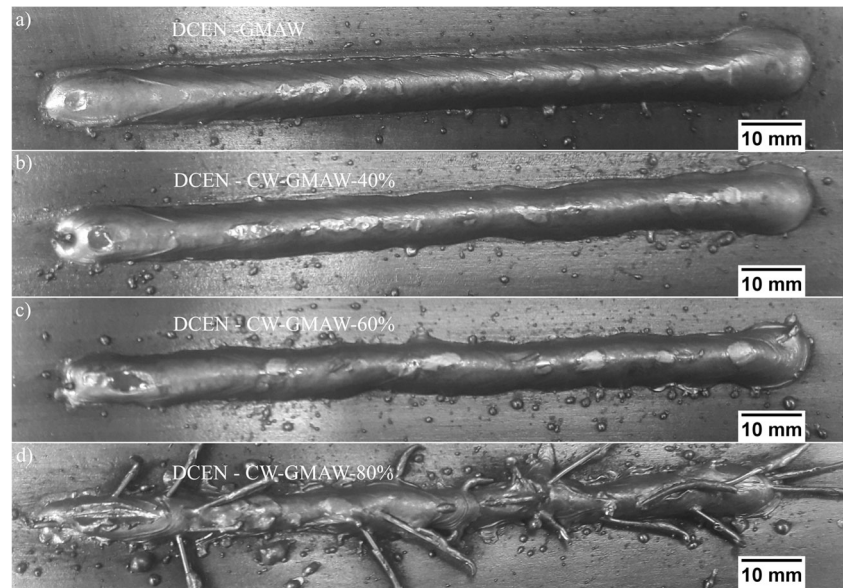
The width of the beads in DCEP is higher than that in DCEN as expected, since in DCEN the convexity is higher due low heat available (refer to Fig. 17b). The wetting angle measured the wetting of the bead to substrate onto which it was deposited. One can see in Fig. 17c that it is higher in DCEN than in DCEP; this is due to the decreased penetration of the former condition. Excessive wetting angles are often factors in welds failing visual inspection. Thus, the parameters with DCEN CW-GMAW-40% represent a limit for the cold wire feed rate.

The average total bead area (Fig. 17d) is an indication of the volume of material deposited, and one can see that it is lower in DCEN than in DCEP for all the cold wire feed rates. This is due to the quantity of spatter in DCEN. Although a higher fraction of wire is melted, only a portion of it is actually deposited onto the substrate. As noted earlier, the spatter due to repelled transfer is a limiting factor in DCEN.

The heat-affected zone (HAZ) area is proportional to the actual heat that diffused across the base metal but was not sufficient to melt it, notwithstanding promoting

Fig. 15 Cross section for positive polarity. (a) Standard GMAW. (b) CW-GMAW-40%. (c) CW-GMAW-60%. (d) CW-GMAW-80%
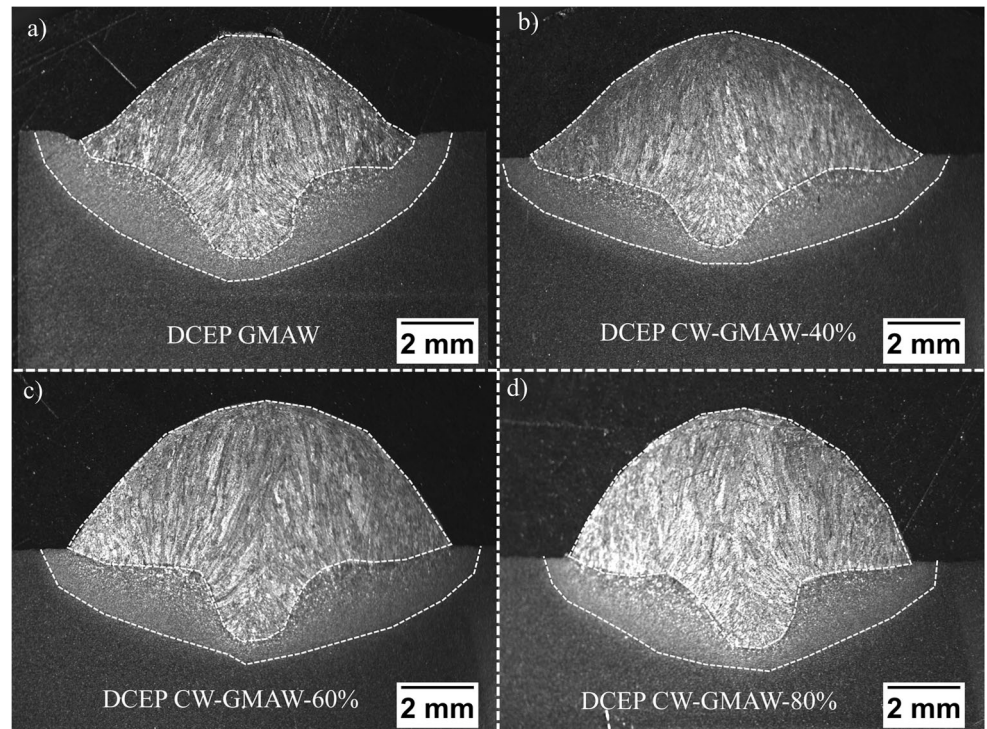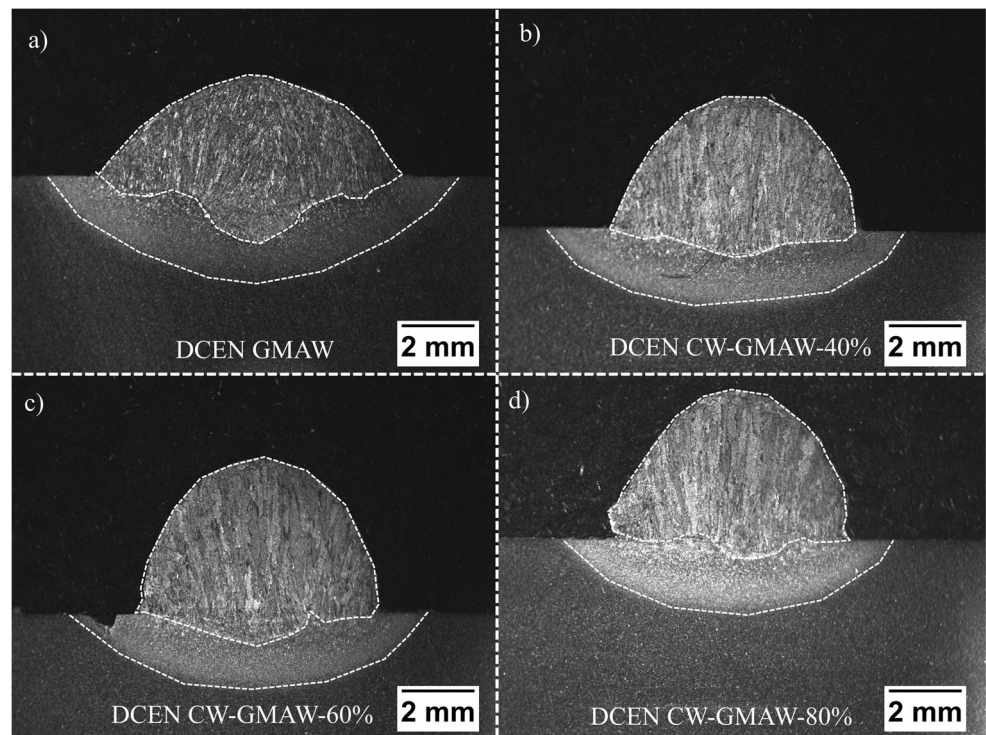
Fig. 16 Cross section for negative polarity. (a) Standard GMAW. (b) CW-GMAW-40%. (c) CW-GMAW-60%. (d) CW-GMAW-80%

metallurgical transformations which is supported by the results by Li et al. [3] whose studies reached the same observation concerning the decrease of the HAZ in DCEN welds.

Thus, by measuring the HAZ area in Fig. 17e, this can provide an indication of the heat actually diffused into substrate. An interesting observation is that at CW-GMAW-40% in DCEN, the area is almost equal to its DCEP counterpart.
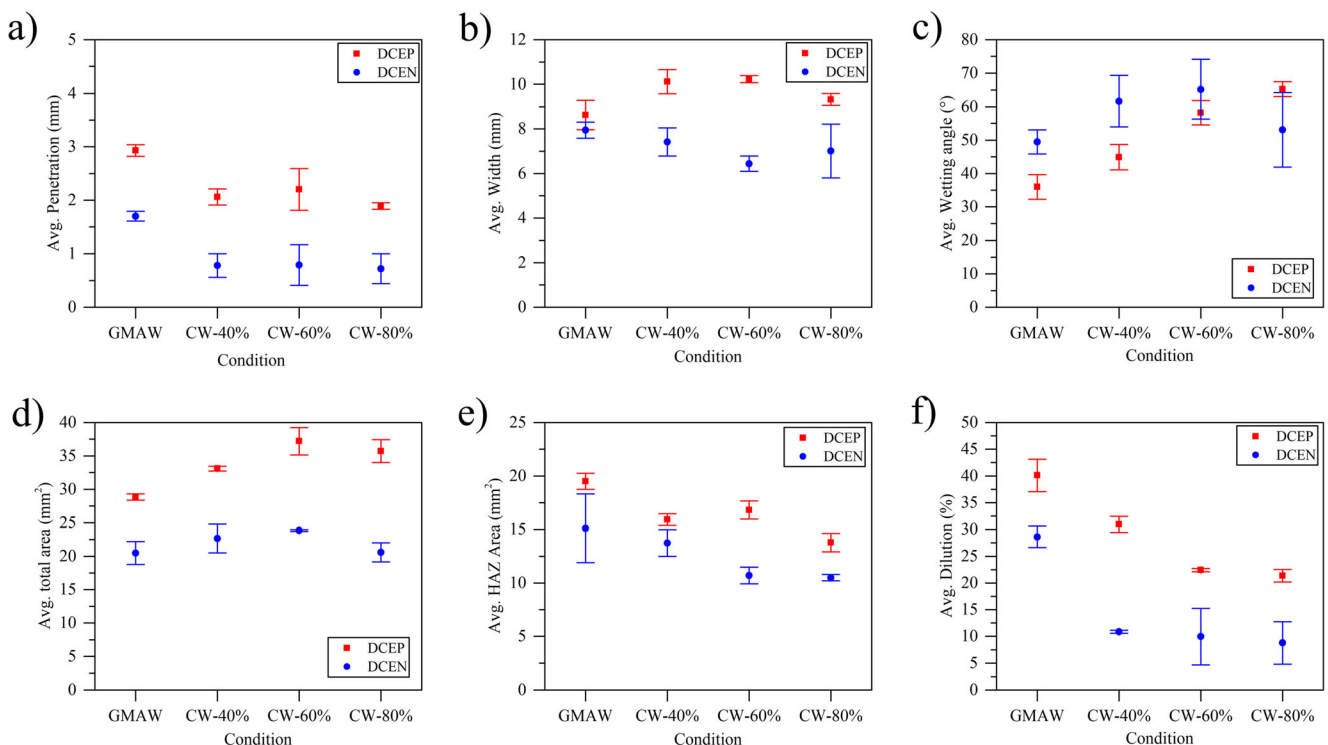

Fig. 17 Geometry parameters of the weld beads and dilution. (a) Depth of penetration. (b) Bead width. (c) Bead wetting angle. (d) Bead total area. (e) HAZ area. (d) Dilution. Average of three cross sections

Another fact worth mentioning is that with the introduction of the cold wire, the variation in HAZ area in DCEN for standard GMAW decreased, indicating that the cold wire promoted less arc wandering motion, making the heat transfer from it to the substrate more consistent.

Dilution is linked to thermal efficiency based on the work of DuPont and Marder [23]; thus, an increase in dilution represents an increase in the power transferred to the substrate in both conditions, DCEP and DCEN; one can see that the dilution decreased compared with the standard GMAW condition, indicating a decrease in heat transferred to the workpiece. This decrease is steeper in DCEN; again, this is due to the low amount of heat available in the melt pool to melt the arc. One observes that the minimum dilution achieved in DCEN is around 10% and that after CW-GMAW-40% the dilution levels off indicating that influence of the cold wire feeding to absorb heat from the melt pool is limited. This value is different from the one obtained in DCEP. In this condition, dilution levels off around 60% of cold wire feed rate reaching a minimum of 25% (refer to Fig. 17f).

4 Conclusions

Bead-on-plate steel welds were performed to study the dynamics of the CW-GMAW in both DCEP and DCEN modes. The following conclusions can be drawn from the presented results:

1. Cold wire GMA welding is feasible both in straight (DCEN) and reverse (DCEP) polarities;
2. The accommodation of the cold wire is function of different heat distribution in the weld pool when the polarity changes, with results suggesting more is heat available in the weld pool in DCEP compared with DCEN;
3. The cold wire feeding is capable of stabilizing the arc for both electrode polarities, although this effect is more pronounced in DCEP;
4. The spatter generated in DCEN affects the deposition as expected, and the cold wire feed rates can increase spatter if the cold wire feed rate exceeds the accommodation limit.

References

1. Norrish J (1974) High deposition MIG-welding with electrode negative polarity. In: 3rd Intl. Conf. on Advances in Welding Processes. The welding Institute, Cambridge, UK., pp 121–128
2. Souza D, de Resende AA, Scotti A (2010) A qualitative model to explain the polarity influence on the fusion rate in the MIG/MAG process. Weld Int 24:934–941. https://doi.org/10.1080/09507110903569032
3. Li P, Hurtig K, Högström M, Svensson LE, Scotti A (2018) A contribution to the study of negative polarity in GMA welding. Int J Adv Manuf Technol 95:2543–2553. https://doi.org/10.1007/s00170-017-1349-z
4. Cho J, Lee J-J, Bae S-H (2015) Heat input analysis of variable polarity arc welding of aluminum. Int J Adv Manuf Technol 81:1273–1280. https://doi.org/10.1007/s00170-015-7292-y
5. Kim K, Chung H (2017) Wire melting rate of alternating current gas metal arc welding. Int J Adv Manuf Technol 90:1253–1263. https://doi.org/10.1007/s00170-016-9384-8
6. Cabral TS, Braga EM, Mendonça EAM, Scott A (2015) Influence of procedures and transfer modes in MAG welding in the reduction of deformations on marine structure panels. Weld Int 29:928–936. https://doi.org/10.1080/09507116.2014.932993
7. Costa ES, Assunção PDC, Dos Santos EBF, Feio LG, Bittencourt MSQ, Braga EM (2017) Residual stresses in cold-wire gas metal arc welding. Sci Technol Weld Join 22:706–713. https://doi.org/10.1080/13621718.2017.1306014
8. Marques LFN, dos Santos EBF, Gerlich AP, Braga EM (2017) Fatigue life assessment of weld joints manufactured by GMAW and CW-GMAW processes. Sci Technol Weld Join 22:87–96. https://doi.org/10.1080/13621718.2016.1194735
9. ASTM (2009) Standard specification for general requirements for steel bars, carbon and alloy, hot-wrought. Changes i:1–16. https://doi.org/10.1520/A0029
10. AWS (2005) AWS A5.28/A5.28M:2005 - Specification for low-alloy steel electrodes and rods for gas shielded arc welding, p 43
11. LEM (1997) Current transducer LF 505-S / SP15, pp 1–2
12. LEM (2017) Voltage transducer LV 100-100 Data Sheet. In: 3
13. do NAS, Batista M de A, do NVC, Scotti A (2007) Assessment of electrical power calculation methods in arc welding and the consequences on the joint geometric, thermal and metallurgical predictions. Soldag Inspeção 12:97–106
14. Kodama S, Ikuno Y, Ichiyama Y, Baba N (2007) Process modeling of short-circuiting GMA welding and its application to arc sensor control. Nippon Steel Tech Rep 95:71–75
15. Hajossy R, Morva I (1994) Cathode and anode falls of arcs with fusible electrodes. J Phys D Appl Phys 27:2095–2101. https://doi.org/10.1088/0022-3727/27/10/016
16. Ribeiro RA, dos Santos EBF, Assunção PDC, Braga EM, Gerlich AP (2018) Cold wire gas metal arc welding: droplet transfer and geometry. Weld J Res Suppl:21
17. Cary HB (1989) Modern welding technology, 2nd edn. Prentice-Hall, Englewood Cliffs, New Jersey
18. Jenney CL, O'Brien A (2004) Welding handbook, 9th edn. AWS, Miami, FL
19. Murray PE, Scotti A (1999) Depth of penetration in gas metal arc welding. Sci Technol Weld Join 4:112–117. https://doi.org/10.1179/136217199101537644
20. Fuerschbach PW (1994) A Dimensionless parameter model for arc welding processes. In: International Conference on Trends in Welding Research, Gatlinburg, TN, USA
21. Mendez PF, Lu Y, Wang Y (2018) Scaling analysis of a moving point heat source in steady-state on a semi-infinite solid. J Heat Transfer 140:081301. https://doi.org/10.1115/1.4039353
22. Scotti A, Rodrigues CEAL (2009) Determination of momentum as a mean of quantifying the mechanical energy delivered by droplets during MIG/MAG welding. Eur Phys J Appl Phys 45:11201. https://doi.org/10.1051/epjap:2008196
23. DuPont JN, Marder AR (1996) Dilution in single pass arc welds. Metall Mater Trans B 27:481–489. https://doi.org/10.1007/BF02914913